

# ADVANCES IN CRYOGENIC ENGINEERING

Proceedings of the International  
Cryogenic Materials Conference—JCMC

*Madison, Wisconsin 16-20 July 2001*

**VOLUME 48B**

*EDITORS*

Balu Balachandran  
Donald Gubser  
KI Ted Hartwig

Ⓢ CD-ROM INCLUDED

**AMERICAN  
INSTITUTE  
OF PHYSICS**

Melville, New York, 2002

AIP CONFERENCE PROCEEDINGS ■ VOLUME 614

# MAGNETIC IMAGING OF YBCO ON RABiTS USING A SQUID MICROSCOPE

A. P. Nielsen<sup>1</sup>, H. R. Kerchner<sup>1</sup>, C. J. Lobb<sup>1</sup>, and P. Barbara<sup>1</sup>

<sup>1</sup>Department of Physics, University of Maryland,  
College Park, MD 20742

<sup>2</sup>Oak Ridge National Laboratory,  
Oak Ridge, TN 37831

<sup>1</sup>Department of Physics, Georgetown University,  
Washington, DC 20057

## ABSTRACT

Using a scanning SQUID microscope we have magnetically imaged YBCO films grown upon Rolling-Assisted Biaxial Textured Substrates (RABiTS). The measurements clearly show a strong (about 3 Oe) and non-uniform spontaneous magnetization due to the Ni-based substrate. The YBCO film on a ferromagnetic substrate cannot be cooled in zero field. We can, however, compare images taken before and after application of a perpendicular magnetic field. Images obtained from the difference between signals in the presence and absence of an applied field are a measurement of the sample magnetization change. For all the values of applied field (from 2 mOe to 100 Oe), we measure screening currents at the sample edges. The hysteretic magnetization shows that some magnetic flux stays trapped by sample defects. AC measurements show both an in-phase screening component of the magnetization and an out-of-phase loss component. Both hysteretic and high frequency (greater than 5 kHz) eddy-current losses are observed. We address the source of the hysteresis and the AC losses by also measuring RABiTS tapes without YBCO and YBCO films on strontium titanate.

## INTRODUCTION

The complex crystal structures, high degree of anisotropy, and short coherence lengths of the cuprate superconductors [1] present serious challenges for researchers seeking applications of these materials. Notwithstanding the difficulties, great progress has been made in fabricating tapes for high-current applications [2-4]. Tapes have achieved current

densities above  $1 \times 10^6$  A/cm<sup>2</sup>, three orders of magnitude higher than carried by conventional electrical wires.

One of the most successful techniques uses rolling-assisted biaxial textured substrates, or RABiTS [2]. In this method, Ni tapes that have a high degree of crystallographic alignment are prepared using rolling and heat treatment. These tapes are then covered with a metal oxide buffer layer and used as substrates for YBCO. While the results obtained are very good, there is experimental evidence that the critical current densities of these composite tapes are not yet at their maximum values [3].

Losses occur in type II superconductors when magnetic flux is present and can move [1]. In order to understand the loss mechanisms in composite tapes, it is useful to image the magnetic-field distribution. This can be done by various means, and there has already been work on YBCO using magneto-optic imaging [3,5] and scanning Hall probes [6]. We have made magnetic images of RABiTS/YBCO using a scanning SQUID microscope, and report preliminary results here. Magneto-optic imaging offers superior spatial resolution and works very well in the moderate to high fields likely to be encountered in applications and scanning Hall probes are also effective in moderate to high fields. By contrast, the SQUID microscope allows excellent field sensitivity, can be used to image samples in zero and low field to determine when flux first enters the sample, and does not require coatings to be deposited on the sample in order to work. The SQUID microscope and other techniques are complementary.

In this paper we first briefly describe two types of sample, RABiTS/YBCO and YBCO grown on STO for comparison. We then describe the scanning SQUID microscope. As a first example of the microscope's capabilities, we show images of STO/YBCO films in the Meissner state, and show that the field distribution agrees with recent theory. We then show data of RABiTS/YBCO, with emphasis on remanence measurements, where samples are scanned after being zero-field cooled, and then scanned again after a field is applied and removed. (The difference between the two images gives important information about how flux is trapped.) By way of comparison, remanence measurements are also shown for STO/YBCO films. Finally, complex AC susceptibility images of RABiTS/YBCO samples are presented.

## EXPERIMENTAL DETAILS

Data from two types of samples will be presented in this paper. The first type of sample is RABiTS coated with YBCO [2,3]. To prevent interdiffusion, which would cause degradation of the YBCO's superconducting properties, sputtered buffer layers are applied to the Ni tape before deposition of YBCO by sputtering. The resulting composites have critical current densities as high as 2 to 3 MA/cm<sup>2</sup>.

Because of the complex structure of the RABiTS/YBCO samples, and the resulting complex magnetic properties, we also looked at YBCO sputtered onto STO substrates under the same conditions. This yields high-quality YBCO films.

The scanning SQUID microscope, shown schematically in FIGURE 1, is of the Black-Wellstood design [7]. A Nb-AlO<sub>x</sub>-Nb SQUID is mounted on the end of a sapphire rod. This rod can be moved in the z direction to bring it close to a second sapphire rod. A second sapphire rod holds the sample, as well as a solenoid to apply a magnetic field and a heater to raise the temperature of the sample. Since the SQUID and the sample are not touching, it is possible to raise the sample temperature to 20 K without significantly heating the SQUID. The sapphire rod attached to the sample is scanned below the stationary SQUID. The SQUID has a white noise of 0.7 pT/Hz<sup>1/2</sup> between 0.5 Hz and 10 kHz. The spatial resolution of the microscope is limited by the SQUID-sample separation, and is typically between 50 μm and 100 μm.

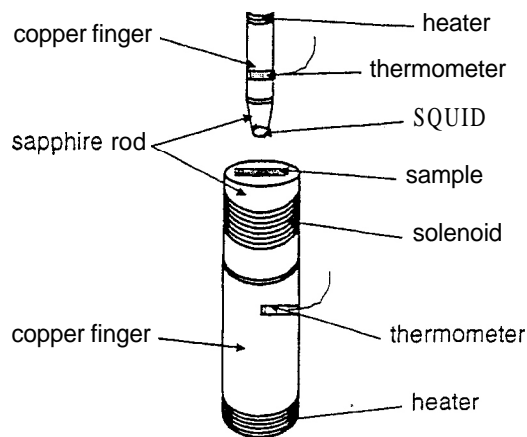


**FIGURE 1.** Schematic diagram of scanning-SQUID microscope. A sapphire tip contains a stationary SQUID that is held above the sample stage. The sample stage is a sapphire rod that is scanned in the x and y directions.

### STO/YBCO SAMPLES IN THE MEISSNER STATE

We first discuss the Meissner state in a 1- $\mu\text{m}$  by 3 mm by 15 mm YBCO film. The film was made by sputtering onto STO and subsequent annealing to form the Y-123 phase. An external magnetic field was applied perpendicular to the film.

To verify that a film is in the Meissner state at a given field, we used the following procedure. We first zero-field cooled the sample, then increased the field to a specific value and then reduced the field to zero again. By comparing images made after the initial zero-field cooling with images made after increasing and then decreasing the field, we determined if any flux had become trapped in the sample. If no flux was trapped in the sample, we concluded that the sample had remained in the Meissner state up to the maximum field that we had applied. We found that the sample remained in the Meissner state for external fields up to 448 mOe.

FIGURE 2 shows the sample in the Meissner state, with  $T=4.2$  K and  $H_{\text{ext}}=224$  mOe.

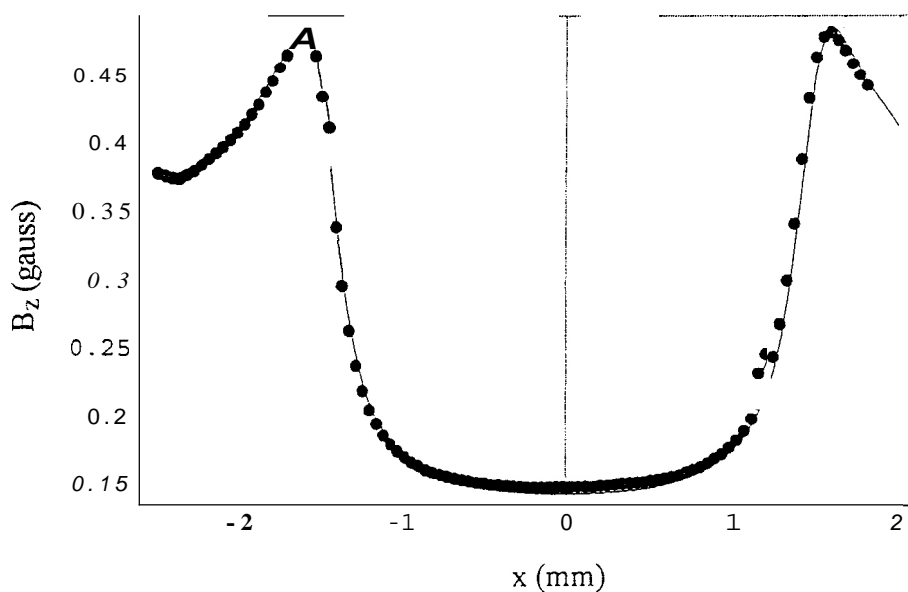


**FIGURE 2.** Comparison of experimental data (solid points) with the magnetic field predicted by Vodolazov and Maaksimov [8] (solid curve).

The figure shows magnetic field as a function of position along a line across the width of the sample. Note the imperfect exclusion of field, which results from the sample being wide and thin, as well as the SQUID's being about 175  $\mu\text{m}$  above the sample. While a detailed comparison of the measured field distribution is beyond the scope of this paper [9], a brief discussion is worthwhile. Comparison with theory is complicated by the fact that the sample is relatively thick ( $d \gg \lambda$ ), keeping it from being two dimensional in the superconducting sense, while the ratio of width over thickness, which is 3000, causes the sample to not be in a simple bulk limit. In spite of the complexity of the problem, Vodolazov and Maksimov [8] provide a theoretical prediction which is in quite good agreement with our image, as can be seen in FIGURE 2.

### REMANENCE IN RABITSNBCO AND STONBCO

We first discuss remanence in STO/YBCO because it is much simpler than RABiTS/YBCO. To make remanence images we first zero-field cool the sample and immediately scan a zero-field reference image. Next, we increase the external field to some value, return the external field to zero, and take another image. The second of the two images shows the remanence. FIGURE 3 contains line-scans of remanent field for three different fields (11.2 Oe, 44.9 Oe, or 57 Oe). It is seen that the flux becomes trapped near the edge of the sample. This is plausible for a sputtered film sample: Defects

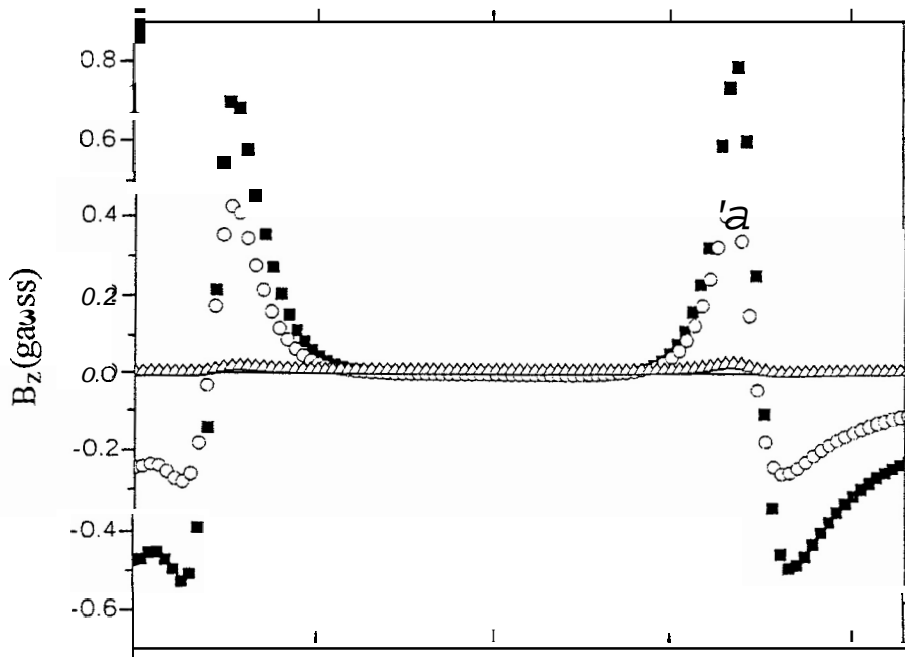


**FIGURE 3.** Line scans from remanence images (see text) of STONBCO film. Maximum field values are 11.2 Oe (open triangles), 44.9 Oe (open circles) and 57 Oe (black squares).

occur throughout the film, causing vortices to be pinned as soon as they enter. This differs quite dramatically from the predictions made where the geometrical barrier is more important than bulk pinning [10]. When the geometrical barrier dominates flux motion, as

is the case in single crystals [10], the flux becomes trapped in the center of the sample, rather than the edges.

The results for the RABiTS/YBCO tapes were more complex. The nickel substrate had a spontaneous magnetization that caused a perpendicular component of magnetic field to be of order 3 Oe, making it impossible to cool the YBCO in zero magnetic field. This means that there were *always* trapped vortices in the sample.

FIGURE 4 shows an image of a RABiTS/YBCO sample cooled in nominally zero magnetic field, that is, there was no current in the copper solenoid in our p-metal shielded Dewar. (Under these conditions, the measured ambient magnetic field in the empty sample space is less than 0.3 mOe). The magnetic structure is quite complex, and the field measured 100  $\mu\text{m}$  above the surface varied over a range of 4.75 G. This image is qualitatively similar to those obtained on bare RABiTS samples without YBCO.

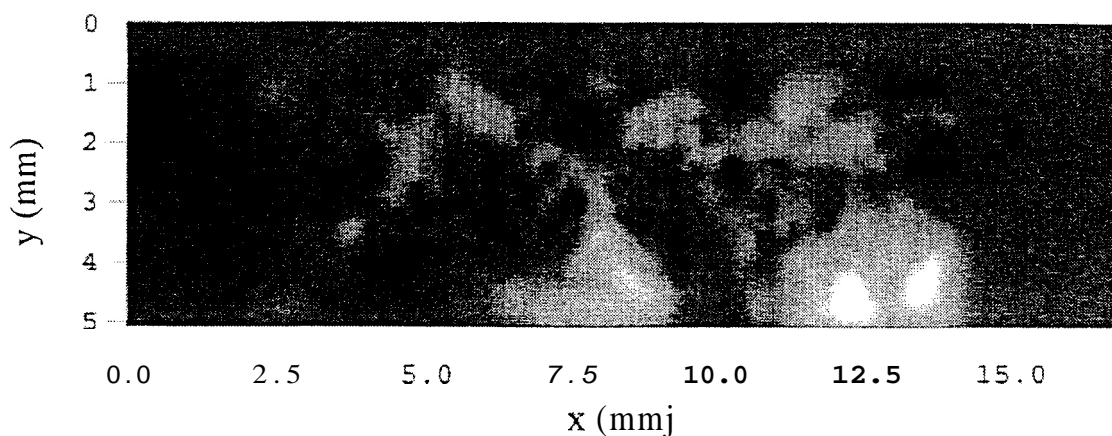


**FIGURE 4.** Magnetic-field image of RABiTS/YBCO. Sample was cooled to  $T=4.2$  K in a field  $H_{\text{ext}} < 0.3$  mOe. Grey scale varies from low (black) to high (white) over a range of 4.75 G.

While the presence of vortices in RABiTS/YBCO would thus seem inevitable, the high critical current densities achieved argue that the vortices must be effectively pinned. To examine this in more detail, we made remanence images.

In FIGURE 5 we show two magnetic-field line scans, one taken immediately after zero-field cooling and one taken after the application and removal of an external field. The peaks in both of the line scans are approximately 100  $\mu\text{m}$  apart, which corresponds roughly to the spacing of holes we observe in the film. Importantly, the size of the peaks changes after the application of the external field (indicated by the arrows in FIGURE 5), indicating that flux has moved into or out of the sample under the influence of the external field. It is this motion of flux, during one cycle of an ac external field, which can cause losses in superconductors that are carrying current.

## AC SUSCEPTIBILITY OF RABiTS/YBCO

In order to understand the basic mechanism involved with loss in YBCO on RABiTS when carrying current, we used the SQUID microscope to perform a local measurement of the AC susceptibility at 1 kHz. We used an EG&G model 5210 lock-in amplifier to measure the applied frequency component in the output from the SQUID electronics. From the lock-in amplifier we acquired two spatially resolved signals, the in-phase component and the out-of-phase component which correspond to the real (loss-less response) and imaginary (lossy response) parts of the AC susceptibility, respectively.

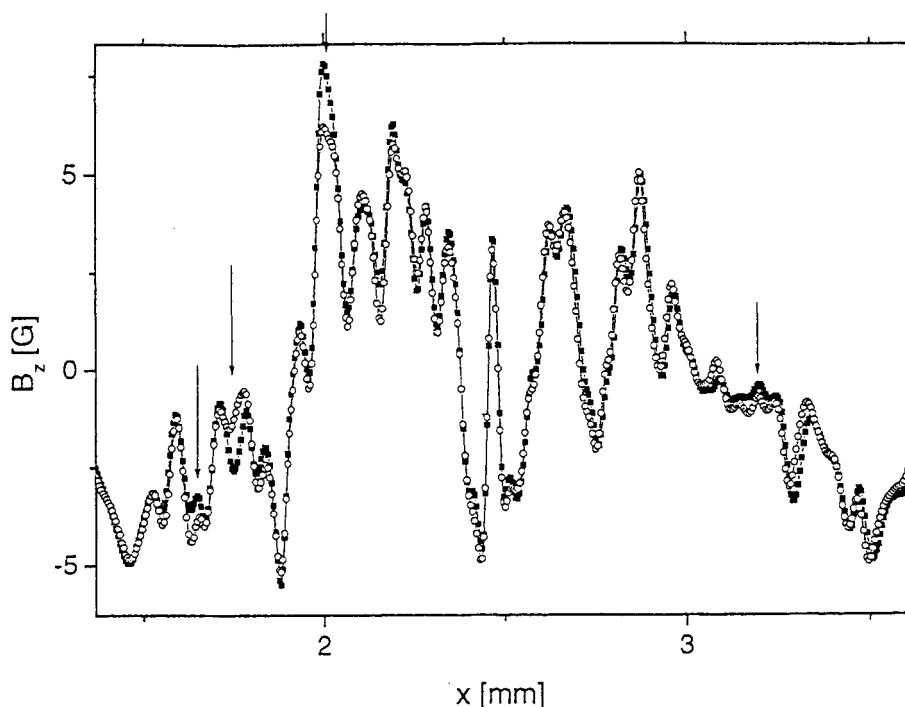


**FIGURE 5.** Line scans of RABiTS/YBCO film after cooling in zero field (open circles) compared to a remanence scan made after cooling in zero field, raising  $H_{ext}$  to 1.16 Oe, and then reducing  $H_{ext}$  to zero again (solid squares). Note that only a few regions (indicated by arrows) have a measurable change in field.

Without YBCO, we would expect to see the eddy current response of the nickel in the loss image. However, the nickel is below (and hence screened by) the YBCO, so we do not expect a response, except in regions where the YBCO fails to screen. In fact this is exactly what we see. In FIGURE 6(a), which shows the loss-free response, there is a light region in the upper right corner of the sample that does not screen the external field. (Darker colors are screening regions in this case because they are closer to zero field.) This same region in FIGURE 6(b), the loss signal, shows the strongest response, indicating that the superconductivity or the pinning in this part of the YBCO is degraded and hence not screening the nickel tape underneath. In addition to this region, there are other regions that have the same correlation between the two images, particularly at the edges of the sample. Furthermore, in the loss signal we see includes some losses inside the YBCO film as well as the Ni eddy current losses. The YBCO losses likely arise from hysteretic vortex motion inside the film.

Using this technique we are able to identify regions where Meissner screening is not occurring and hence the YBCO is either weakly superconducting, or the vortices are very weakly pinned. Additionally we can identify regions of hysteretic response, indicating that vortices are moving about causing loss. From this it will be possible to examine those particular regions of the sample in detail and determine how to improve the superconductivity in those regions.

## SUMMARY AND CONCLUSIONS

A scanning SQUID microscope has been used to identify regions in a YBCO film grown on RABiTS substrates to determine which regions of the film are causing losses to occur. DC hysteresis measurements indicate that regions inside the superconductor contain losses correlated with holes in the superconducting film. In addition, scanning **AC** susceptibility measurements indicate that some regions near the edge of the YBCO film are

not optimal: They are too thin, have weak pinning, or for some other reason are weakly superconducting. There are also hysteretic losses associated with some regions interior to the film.

Furthermore, measurements of YBCO on STO have allowed us to measure the shielding current distribution of a thick superconducting film in the Meissner state. We obtain results that are in good agreement with the theoretical distribution of Vodoiazov and Maksimov [8]. This current distribution is remarkably different from YBCO on RABiTS. In fact, no Meissner state distribution could be measured on the RABiTS/YBCO samples because of the magnetization of the Ni substrates.

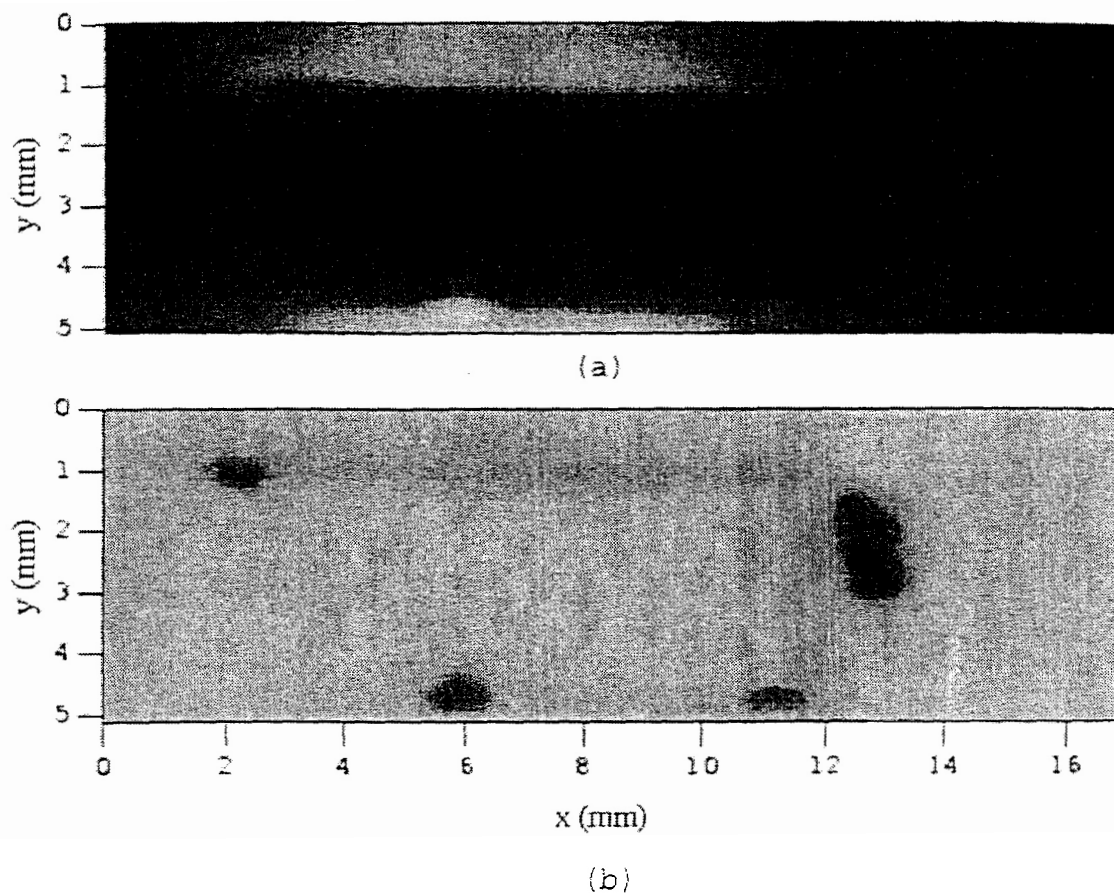


**FIGURE 6.** AC susceptibility response at 1 kHz, taken with the SQUID at a height of 50 micrometers. Images of the (a) in phase (-0.015 G (black) to 0.25 G (white)) and (b) out of phase (-0.045 G (black) to 0.01 G (white)).

## ACKNOWLEDGEMENTS

Supported by NSF Grant No. DMR-9732800, AFOSR Grant No. F496209810072, the Maryland Center for Superconductivity Research, and DOE Contract No. DE-AC05-00OR22725 with Oak Ridge National Laboratory, Managed by UT-Battelle, LLC.

## REFERENCES

1. Tinkham, M., *Introduction to Superconductivity*, McGraw Hill, New York, 1996, pp. 316-382.
2. Goyal, A., Norton, D. P., Kroeger, D. M., Christen, D. K., Paranthaman, M., Specht, E. D., Budai, J. D., He, Q., Saffian, B., List, F. A., Lee, D. F., Hatfield, E., Martin, P. M., Klabunde, C. E., Mathis, J., Park, C., *J. Mat. Res.* **12**, pp. 2924-2940 (1997).

3. Feldmann, D. M., Reeves, J. L., Polyanskii, A. A., Kozlowski, G., Biggers, R. R., Nekkanti, R. M., Nekkanti, R. M., Maartense, I., Tomsic, M., Barnes, P., Oberly, C. E., Peterson, T. L., Babcock, S. E., and Larbalestier, D. C., *Appl. Phys. Lett.* **77** pp. 2906-2908 (2000).
4. Feldmann, D. M., Reeves, J. L., Polyanskii, Goyal, A. A., Feenstra, R., Lee, D. F., Paranthaman, M., Kroeger, D. M., Christen, D. K., Babcock, S. E., and Larbalestier, D. C., *IEEE Trans. Appl. Supercon* **11**, pp. 3772-3775 (2001).
5. Johansen, T. H., Baziljevich, M., Bratsberg, H., Galperin, Y., Lmdelof, P. E., Shen, Y., and Vase, P., *Phys. Rev. B* **54**, pp. 16264-16269 (1996).
6. Ferdeghini, C., Giannini, E., Grassano, G., Marre, D., Pallecchi, I., and Siri, A. S., *Physica C* **294**, pp. 233-242 (1998).
7. Black, R. C., Mathai, A., Wellstood, F. C., Dankster, E., Miklich, A. H., Nemeth, D. T., Kingston, J. J., and Clarke, J., *Appl. Phys. Lett.* **62**, pp. 2128-2130 (1993).
8. Vodolazov, D. Y. and Maksimov, I. L., *Physica C* **349**, pp. 125-138 (2001).
9. Nielsen, A. P., Lobb, C. J., Barbara, P., and Kerchner, H. R., manuscript in preparation.
10. Zeldov, E., Larkin, A. I., Geshkenbein, V. B., Konczykowski, M., Majer, D., Khaykovich, B., Vinokur, V. M., and Shtrikman, H., *Phys. Rev. Lett.* **73**, pp.1428-1431 (1994).